Pressure dependence of the crystal structure of $CuGeO_3$ to 6.2 GPa by neutron diffraction

M. Braden
Forschungszentrum Karlsruhe, INFP, Postfach 3640, D-76021 Karlsruhe, Germany
and Laboratoire Léon Brillouin, CE-Saclay, 91191 Gif-sur-Yvette, France

B. Büchner
II. Physikalisches Institut, Universität zu Köln, Zülpicher Strasse 77, D-50937 Köln, Germany

S. Klotz
Physique des Milieux Condensés, (CNRS URA 782), Université Pierre et Marie Curie B77, 4 place Jussieu, F-75252 Paris, France

W. G. Marshall
ISIS Facility, Rutherford Appleton Laboratory, Chilton, Didcot OX11 0QX, United Kingdom

M. Behruzi and G. Heger
Institut für Kristallographie, RWTH-Aachen, Jägerstrasse 17-19, D-52056 Aachen, Germany
(Received 19 February 1999; revised manuscript received 30 April 1999)

The structure of the spin-Peierls compound $CuGeO_3$ has been analyzed by time-of-flight neutron powder diffraction as a function of external pressure. The structural changes allow us to explain the strong pressure dependence of the magnetic susceptibility most likely related to the pronounced pressure-induced increase of the spin-Peierls transition temperature. The structural changes induced by Si substitution are found to be opposite to those observed upon applying external pressure. [S0163-1829(99)11037-3]

I. INTRODUCTION

The discovery of the spin-Peierls (SP) transition, a dimerization of spin-$\frac{1}{2}$ magnetic chains associated with a lattice distortion, in $CuGeO_3$ (CGO) has attracted a lot of attention since its rather simple crystal structure permits detailed microscopic experimental studies.[1,2] It is well known that applying external pressure drastically influences the spin-Peierls transition in CGO. From the pronounced anomalies of the thermal expansion coefficients at the transition temperature T_{SP} large, strongly anisotropic pressure derivatives of T_{SP} are derived. For example, a pressure dependence of 4.5 K/GPa may be obtained from thermodynamic relations, i.e., for the thermodynamic limit $p \rightarrow 0$.[3,4] This pressure derivative was later confirmed at finite pressures from measurements of the magnetic susceptibility,[5] from neutron-diffraction studies on the nuclear superstructure reflections in the dimerized phase[6] as well as from Raman light-scattering experiments.[7,8] The latter indicate minor deviations from a strictly linear increase of T_{SP}, which becomes visible at high pressures of several GPa. The pressure dependence of the magnetic excitation spectrum in the dimerized phase of CGO was studied in detail. From their neutron-scattering experiments Nishi *et al.*[9] found a drastic enhancement of the spin gap Δ with increasing p, which is even larger than the (normalized) increase of T_{SP}, i.e., the ratio Δ/T_{SP} increases with increasing p. The observed increase of T_{SP} upon pressure should be considered as quite anomalous compared to typical magnetic transitions. A detailed knowledge of the pressure dependencies of the different magnetic coupling parameters promises an insight into the mechanism of the SP transition in CGO.

An investigation of these pressure dependencies at high temperatures is important in order to investigate the spin-lattice coupling, which is a precondition for the SP transition. Experimentally a change of the antiferromagnetic coupling as a function of structural parameters can be inferred from the pressure dependence of the magnetic susceptibility.[5] These data and also measurements of the dispersion curves[9] signal a decrease of the magnetic coupling constant J along the chains with increasing hydrostatic pressure. Magnetostriction data show, in addition, a strong anisotropy of the spin-lattice coupling,[10–12] i.e., the uniaxial pressure derivatives of J differ in signs and sizes. The magnetic interaction described by J depends sensitively on structural parameters, and may be even quantitatively deduced from it. Therefore, a detailed knowledge of the high-pressure structure is highly desirable, and will be a test for the proposed J-structure relations.[13,14]

Results of high-pressure crystal structure studies were already available before the discovery of the SP transition. Adams *et al.* performed x-ray-diffraction measurements up to 22 GPa.[15] Below 6.6 GPa they observed a strongly anisotropic compressibility similar to the pronounced anisotropy of the thermal expansion. The energy dispersive diffraction technique did not allow Adams *et al.* to perform a quantitative analysis of the reflection intensities. Under the assumption of rigid tetrahedra and CuO_4 units, Adams *et al.* deduced a rotation of the CuO ribbons around the c axis. Above 6.6 GPa, a structural phase transition occurs.

Due to the renewed interest in CGO two crystallographic studies have been performed more recently. Based on the pressure dependence of a few superstructure reflection intensities in the dimerized phase, Katano *et al.*[6] calculated the

shift of the dimerization distortion upon pressure. However, already the ambient pressure distortion does not agree with a more detailed study.[13] Upon pressure increase Katano *et al.* observe a reduction of the positional shift of the Cu site along *c* and that of the oxygen closer to Cu (O2) along *a*, whereas the shift of O2 along *b* increases. The Cu-O-Cu bond angle η, which appears to dominate the magnetic interaction in CGO, shows a smaller alternation upon pressure, thereby weakening the modulation of the magnetic interaction. Furthermore, they found that the average value of η increases under pressure.

The pressure dependence of the undistorted *Pbmm* structure was analyzed by Bräuninger *et al.* at room temperature using a diamond-anvil cell and synchrotron radiation.[16] This group, too, reported a slight increase of η under pressure; however, their experimental error of more than 1° is certainly insufficient for analyzing the extreme sensitivity of the magnetic interaction on this angle. Other structural parameters shift rapidly enough in order to be detected by this method, however. Bräuninger *et al.* confirmed the rotation of the CuO_2 ribbons around the *c* axis together with a strong reduction of the CuO1 bond length, as suggested by Adams *et al.*[15]

In order to obtain a more quantitative knowledge about the crystal structure of CGO under pressure and its relevance for the magnetic interaction parameters, we have performed further crystallographic studies using powder neutron diffraction which permit a more precise analysis of the oxygen positions. In addition we compare the pressure-induced effects to those arising from the substitution of the Ge by the smaller Si.

II. EXPERIMENT

All diffraction data were taken at the POLARIS and PEARL/HiPr time-of-flight (TOF) diffractometers of the ISIS Neutron Facility at the Rutherford Appleton Laboratory using the Paris-Edinburgh cell. This device permits a sample volume of ~ 100 mm^3 to be compressed to 10 GPa.[17] Fluorinert (3M) was used as pressure transmitting medium. The Paris-Edinburgh cell with tungsten-carbide (WC) anvils does not permit a direct determination of the pressure by optical methods. We have determined the pressure from the rapidly varying lattice constant *b* by comparison to Ref. 16. At a small cell load of 3*t*, which is necessary in order to seal the cell without yielding a pressure on the sample, a reference diffraction pattern was recorded with reduced counting time. Patterns were then collected with progressively longer counting times at various loads up to a maximum of 125*t*. This strategy was used to offset the partial loss of signal caused by the closing down of the anvils, which reduces the effective sample volume visible to the detectors. Due to the large compressibility of CGO this effect turned out to be rather strong in our experiment.

The data were used for refining the structural model corresponding to the *Pbmm* phase of CGO.[13] Contaminating reflections originating from the WC anvils were treated as a secondary phase in the refinements. For patterns obtained at pressures above 6.6 GPa, structural models corresponding to several subgroups of *Pbmm* were refined in order to describe the high-pressure phase of CGO. All refinements were performed using the GSAS program package.[18] Parts of the observed diffraction patterns together with their calculated profiles are shown in Fig. 1; the results of the refinements are given in Table I. The absolute values of the lattice parameters determined with the TOF technique depend sensitively on the position of the sample. Hence, due to small uncertainties (~ 5 mm) in the positioning of the large pressure cell with respect to the instrument reference point, the measured lattice parameters show a slight reduction of -0.1% when compared with the results of earlier studies[13] or those at ambient conditions, see Table II and below.

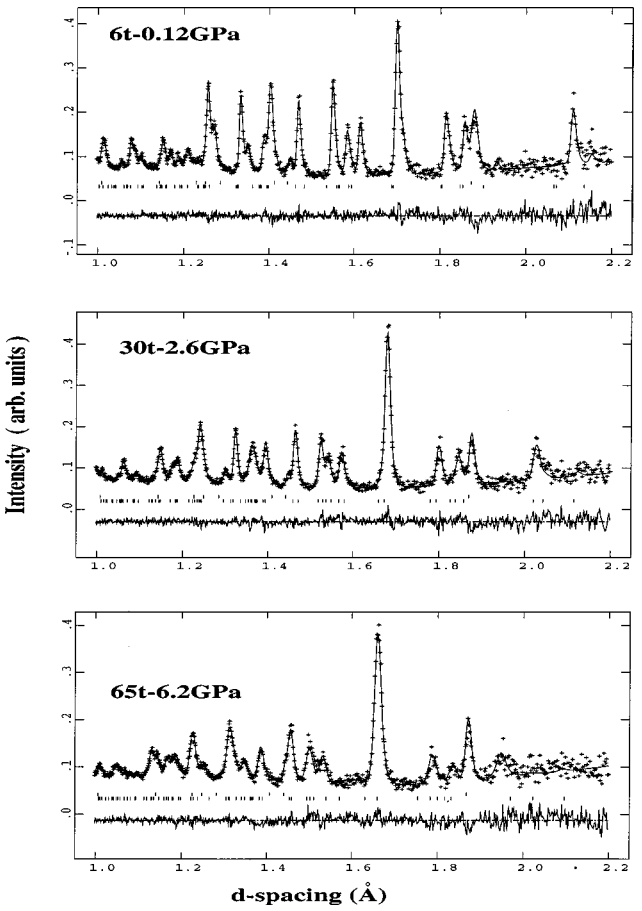

FIG. 1. Parts of the neutron-diffraction patterns of CGO obtained at different pressures, with the crosses designating the data and the lines the calculated and the difference spectra corresponding to the *Pbmm* structural model at 0.12, 2.58, and 6.16 GPa, respectively. The two sets of vertical bars indicate the positions of the Bragg reflections due to the CGO (below) and WC (above) phases.

The stoichiometric sample used for the high pressure experiments and the partially Si-substituted sample were analyzed on the PEARL/HiPr diffractometer under ambient conditions. These data were used for refining the standard structural model in space group *Pbmm*; see Table II. All error bars given in tables and figures are taken from the refinement procedure.

III. RESULTS AND DISCUSSION

Pressure dependence of the Pbmm structure . The pressure dependences of the orthorhombic lattice parameters de-

TABLE I. Results of the structure refinements at different pressures. The estimated standard deviations in the last digits are given in parentheses; mean-square displacements are given in Å ^{2}. U_{12} of O2 was fixed to zero.

Load	3*t*	6*t*	12*t*	21*t*	30*t*	50*t*	65*t*
pressure (GPa)	0	0.12(1)	0.91(1)	1.84(1)	2.58(1)	4.67(1)	6.16(1)
R_{wp} (%)	9.6	5.46	5.94	5.42	5.65	5.70	5.48
χ^2	1.41	1.26	1.16	1.26	1.32	1.30	1.27
a (Å)	4.786(1)	4.7843(4)	4.7715(9)	4.7565(5)	4.7464(5)	4.7223(7)	4.7170(9)
b (Å)	8.449(2)	8.4287(8)	8.3058(9)	8.1821(9)	8.0959(11)	7.8934(16)	7.776(2)
c (Å)	2.9349(4)	2.9336(2)	2.9318(2)	2.9279(2)	2.9236(2)	2.9137(3)	2.9071(4)
V (Å ^{3})	118.68	118.30	116.19	113.95	112.34	108.61	106.63
Cu U_{iso}	0.012(1)	0.010(1)	0.0105(8)	0.0114(8)	0.0093(8)	0.0103(9)	0.010(1)
Ge *x*	0.0767(11)	0.0744(7)	0.0690(7)	0.0634(7)	0.0595(7)	0.0515(9)	0.0461(10)
U_{iso}	0.006(1)	0.0076(8)	0.0066(8)	0.0063(7)	0.0077(7)	0.0075(8)	0.0094(10)
O1 *x*	0.8649(15)	0.8640(9)	0.8587(9)	0.8539(9)	0.8496(9)	0.8425(12)	0.8323(13)
U_{iso}	0.0105(16)	0.0079(9)	0.0070(9)	0.0085(9)	0.0085(9)	0.0136(13)	0.009(2)
O2 *x*	0.2848(13)	0.2836(8)	0.2766(9)	0.2747(8)	0.2733(9)	0.2672(9)	0.2644(10)
y	0.0825(8)	0.0830(5)	0.0814(6)	0.0787(5)	0.0775(5)	0.0753(7)	0.743(8)
U_{11}	0.024(4)	0.017(2)	0.014(2)	0.010(2)	0.021(2)	0.018(2)	0.011(3)
U_{22}	0.022(3)	0.023(2)	0.027(3)	0.022(2)	0.018(2)	0.022(3)	0.022(3)
U_{33}	0.001(2)	0.003(2)	0.002(2)	0.005(2)	0.015(2)	0.009(2)	0.05(2)

termined in Refs. 15 and 16 do not agree very well with each other. Adams *et al.* obtained a smaller compressibility of *b* and larger ones for *a* and *c*, which is most probably due to some uniaxial pressure components in their experiment. A nonfluid pressure medium might be unable to follow the strong contraction of CGO along *b* due to shear forces as discussed first in Ref. 7. In addition to the viscosity of the medium, the real structure of the grains in the polycrystalline sample appears to be important in this context. Larger grains or single crystals will necessitate the use of a fluid medium in order to obtain hydrostatic conditions. Furthermore, a high filling of the cell with the polycrystalline sample implies a bridging between the grains resulting in rather complicated local pressure components. The lattice constants observed in our experiment correspond well to those of Bräuninger *et al.*[16] (note that the pressure values given in Table I have been determined by comparing the *b* parameter to these results); in particular we obtain the same strong reduction of *b* just below the transition to the high-pressure phase. This proves that the freezing of the Fluorinert in our powder experiment does not lead to pronounced non–hydrostatic compression, which is further supported by the nature of the high-pressure phase observed above 6–7 GPa.[19]

In agreement with all previous work, we find the *Pbmm* structure up to pressures of ~6.6 GPa. Furthermore, we confirm the pronounced variation of the atomic parameters; the obtained bond lengths and angles are shown in Figs. 2 and 3. As observed as a function of temperature[13,20] and as reported previously,[15,16] the CuO_2 ribbons are rotated around the *c* axis. The angle τ decreases with increasing pressure, i.e., the ribbons become more parallel to the *a* axis. A temperature reduction by 100 K (Ref. 20) corresponds to an increase of the pressure by approximately 0.5 GPa, which demonstrates the stronger variation achieved by external pressure. Compared to the previous x-ray experiments we obtain a higher precision especially for the oxygen positions permitting a quantitative analysis of these effects. The rotation angle of the ribbons increases continuously in the examined pressure range, but it exhibits pronounced nonlinearities above 2 GPa. The flattening of the pressure dependence should be related to the limited stability of the *Pbmm* structure in accordance with the observed phase transition near 6.6 GPa.[7,8,15,16] Similar to the temperature-dependent observations, only the Cu-O1 bond is strongly compressed under pressure, and the reduction of this bond by 10% appears anomalously large. The Cu-O1 length observed at high pressure is comparable to those observed in some high-T_c cuprates which are usually considered as being sixfold coordinated. Therefore, one may conclude that the coupling between the zigzag layers in CGO becomes enhanced at high pressure. The pronounced volume compressibility is fully explained as an approach of these zigzag planes, with an accompanying increase of the undulation described by the angles τ or δ.

The rigid components of the $CuGeO_3$ structure, the CuO_4 squares and GeO_4 tetrahedra, are less affected by pressure. The Ge-O distances are more compressed than the Cu-O2 distance, in disagreement with the more covalent nature expected for the Ge bonds. This indicates some internal constraints imposed by the *Pbmm* symmetry. A pronounced shortening is further observed for the O2-O2 tetrahedron edge parallel *b* (related to the bond angle γ), which contrasts to the absent thermal contraction of this length.

Discussion of the pressure dependence of exchange parameters and T_{SP}. The behavior of the bond angles O2-Cu-O2, η, and O2-O2-Ge, δ, appears to be particularly interesting, as these angles dominate the magnetic interaction in CGO. For CuO_2 chains with a 90° bond angle, and neglecting the influence of side-groups, one expects a ferromagnetic interaction between neighboring Cu spins, since there is no antiferromagnetic superexchange in the 90° Cu-O-Cu connection. In order to render the interaction antiferromagnetic,

TABLE II. Results of the structure refinements on CGO and $CuGe_{0.76}Si_{0.24}O_3$ at ambient conditions. The estimated standard deviations in the last digits are given in parentheses; mean-square displacements are given in Å ^{2}.

	$CuGeO_3$	$CuGe_{0.76}Si_{0.24}O_3$
R_{wp} (%)	2.86	2.75
χ^2	9.031	9.427
a (Å)	4.8034(2)	4.7767(2)
b (Å)	8.4786(2)	8.5345(3)
c (Å)	2.94452(5)	2.9192(1)
V (Å ^{3})	119.92	119.02
Cu U_{11}	0.0175(8)	0.0106(9)
U_{22}	0.0136(6)	0.0101(6)
U_{33}	0.0023(5)	0.0040(6)
U_{12}	0.0069(5)	0.0057(5)
Ge x	0.0754(2)	0.0792(2)
U_{11}	0.0093(6)	0.0174(8)
U_{22}	0.0084(6)	0.0190(7)
U_{33}	0.0020(5)	0.0089(7)
O1 x	0.8662(3)	0.8777(4)
U_{11}	0.0106(9)	0.0215(12)
U_{22}	0.0165(8)	0.0084(8)
U_{33}	0.0004(7)	0.0027(9)
O2 x	0.2826(2)	0.2855(2)
y	0.0836(1)	0.0862(1)
U_{11}	0.0163(8)	0.0152(9)
U_{22}	0.0143(6)	0.0130(6)
U_{33}	0.0053(5)	0.0025(6)
U_{12}	0.0090(5)	0.0122(6)

this degenerate arrangement has to be distorted either by elongating the CuO_4 squares or by hybridization with neighboring Ge atoms. This has been discussed in detail in Refs. 13 and 14. In CGO both effects depend sensitively on the angles: the elongation is directly described by η and the hybridization influenced by δ. The hybridization effect should be largest for the Ge lying in the plane of the CuO_2 ribbons, and should vanish if the Ge-O2 bond is perpendicular to the ribbons. Several attempts have been made to determine the microscopic couplings between J and these angles.[13,14] Qualitatively, it is obvious that J increases with increasing η and δ. Microscopic analyses by band structure calculations yield $\partial J/J\partial\eta = 0.44$(1/deg) and 0.13(1/deg) in Refs. 13 and 14, respectively, and $\partial J/J\partial\delta = 0.011$(1/deg) and 0.006(1/deg). The bond angle dependences deduced from magnetostriction data[21] amount to $\partial J/J\partial\eta = 0.10$(1/deg) and $\partial J/J\partial\delta = 0.01$(1/deg). Due to the large uncertainties in the parameters used for the microscopic calculations and the rough estimations made in Ref. 21, the agreement between the different attempts appears reasonable.

The observed decrease of δ agrees with previous reports. However, in contrast to the previous studies,[6,16] we obtain a weak decrease of η. Due to the strong sensitivity of the magnetic interaction on this angle, the small decrease of η still induces a large decrease of J, which is enhanced by the decrease of δ. Using the angular dependences reported in Refs. 13, 14, and 21 for the derivative one obtains $\partial J/J\partial P$ -0.085, -0.033, and -0.029 (1/GPa) respectively. This result may be compared to the experimentally determined pressure dependencies of J. Takahashi *et al.* analyzed the magnetic susceptibility, and obtained $\partial J/J\partial P = -0.07$(1/GPa). Fabricius *et al.* deduced[12] $\partial J/J\partial p = -0.08$(1/GPa) from magnetostriction data.[4] The agreement between the different techniques appears rather satisfying; furthermore, these results may be fully explained by the structural changes, confirming rather strong coupling constants. The effect of the side groups becomes enhanced due to the pronounced variation of δ upon pressure. A more quantitative analysis of the pressure dependence, however, needs the incorporation of the changes of the bond lengths, which vary significantly upon pressure. Recently, Werner *et al.*[22] obtained microscopic coupling constants from a random-phase-approximation treatment of the structural distortion below T_{SP} and the polarization patterns of the involved phonon modes. This rather more complete set of parameters is, again, in good agreement with experiment.[22] The influence of the bond-lengths on $J(P)$ gives corrections of the order of 10% which almost cancel each other. Note that for the calculation of the modulation of J in the dimerized phase below T_{SP}, the effects of the bond distances can be completely neglected. Also the influence of the δ modulation is much smaller on the SP distortion[13] than on the $J(P)$ curve. In the Cross-Fisher theory of the SP transition,[23] the value of J does not enter directly the expression for T_{SP},

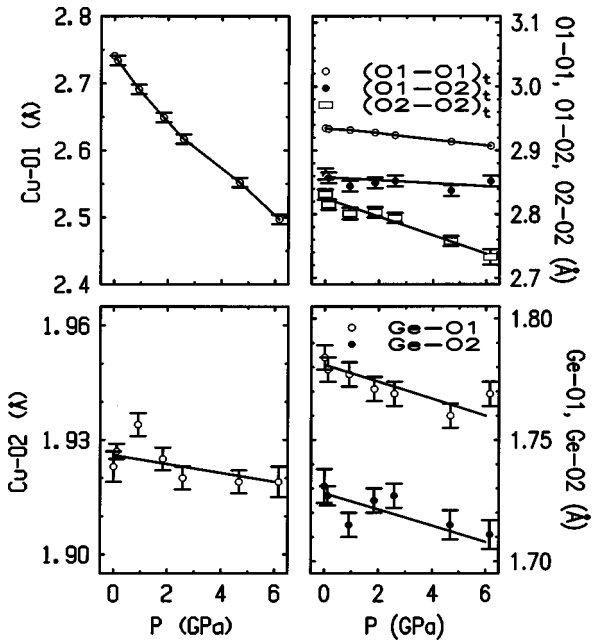

FIG. 2. Pressure dependence of several bond distances in CGO. All O-O distances correspond to bonds within one GeO_4 tetrahedron.

$$T_{SP} \propto \frac{4g^2}{\pi\Omega_0^2}, \tag{1}$$

with Ω_0^2 the bare phonon frequency and g the spin-phonon coupling constant. This theory was recently applied to the case of CGO, where four phonon modes are involved.[24] van Loosdrecht *et al.*[8] have analyzed the pressure dependence of the additional modes appearing in Raman scattering in the

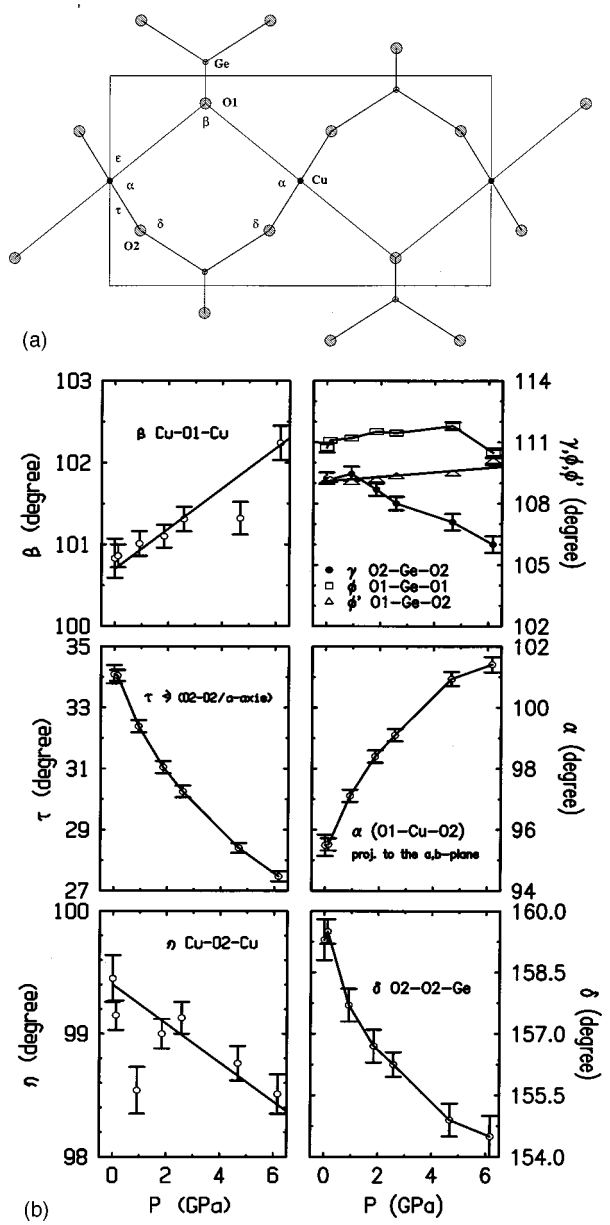

FIG. 3. (a) Schematic picture of the CGO structure projected to the a,b plane, indicating the definitions of several bond angles. (b) Pressure dependence of the bond angles in CGO within the $Pbmm$ phase.

SP phase. In particular, the line at 228 cm^{-1}, which was later identified as arising from the phonon mode most involved in the dimerization,[25] decreases by -2% GPa. Therefore, the elastic energy due to the distortion is reduced upon pressure. This effect yields an increase of T_{SP} but appears to be far too small in magnitude. Furthermore, there is no indication that the coupling constants g in Eq. (1) exhibit a pressure dependence of the order of 15% per GPa.

Within the Cross-Fisher theory, one may not relate the large T_{SP} enhancement to the decrease of the magnetic coupling. Instead, one should argue that the decrease of J results in an enlarged ratio between the frustrating next-nearest neighbor J' and the nearest neighbor interactions. The frustration through the next-nearest-neighbor interaction is now well established to be essential for an understanding of the magnetic susceptibility[26,27,12] and other properties of CGO. Including J' in the Cross-Fisher theory should alter the proportionality in Eq. (1). The exchange along the path for next-nearest-neighbor interaction Cu-O2-O2-Cu might slightly increase due to the reduced O2-O2 distance at high pressures. However, the contribution of this effect on the frustration ratio should be negligible compared to the large enhancement due to the reduction of J upon pressure. Direct evidence of an enhanced frustration-ratio upon pressure was reported in the neutron-scattering study by Nishi *et al.*[9] which, furthermore, clearly demonstrates the higher spin gap.

The fact that the frustration enhances the spin gap[28] in the dimerized phase, or even induces the spin gap if high enough, may qualitatively explain the increase of T_{SP}, since the energy gain due to the opening of the spin gap has to overcome the elastic energy. If the magnetic energy gain increases through the enhanced frustration J'/J, the transition may occur at higher temperature. Furthermore, recent density matrix renormalization-group (DMRG) calculations by Klümper *et al.*[29] confirm this picture, leaving all parameters unchanged; T_{SP} definitely increases with frustration. The direct dependence of the T_{SP} on the magnetic coupling parameters was also deduced from the anisotropic uniaxial pressure dependencies and the magnetostriction data.[10]

Structure of Si-containing CGO. There has been a controversy about the influence of Si doping on the SP phase transition. In polycrystalline samples, Oseroff *et al.* observed that 10% of the Ge can be replaced by Si without a pronounced reduction of T_{SP}.[30] In contrast the single crystal studies by Renard *et al.* show a drastic reduction of T_{SP} upon Si doping: for a Si concentration of just 2% the SP transition is completely suppressed in single crystals.[31] However, even in samples with a high Si content a short-range dimerization order persists. A detailed investigation was performed by Weiden *et al.*,[32] who suggested that the differences would be due to a nonstoichiometric oxygen occupation in the case of the single crystals, which are synthesized at higher temperatures. Apart from an increase of the b parameter and a reduction in a and c,[32] relatively little information has been available concerning the structural effects of Si doping. The linear relationship which remains valid even at higher Si concentrations proves that the Si really substitutes for Ge in the CGO structure.

The Si-containing sample obtained by the standard preparative technique and the stoichiometric sample used for the pressure experiments were studied under ambient conditions, which yielded much improved statistics over the experiments in the pressure cell described above. A part of the diffraction pattern obtained on the PEARL/HiPr diffractometer is shown in Fig. 4. The corresponding structural results are given in Table II. Electron microsonde analyses revealed a Si content of 27(3)%, reproducible at several positions on the surface of the sample. A comparable Si concentration results, furthermore, from a comparison of the lattice parameters (see Table II) to those previously published,[32] $x=0.21(2)$. Si and Ge possess rather different scattering lengths for thermal neutrons, which allow an accurate determination of the Si concentration in the structural refinements. The obtained value of 24(1)% confirms the other techniques.

The cell volume of the Si-containing sample is reduced with respect to the stoichiometric compound, whereas the b parameter is strongly increased. This clearly demonstrates

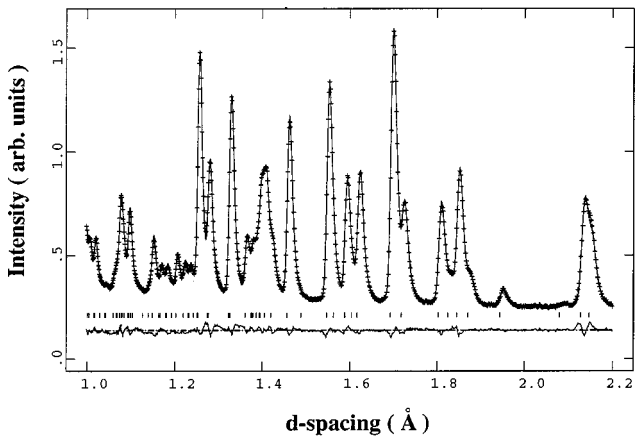

FIG. 4. Part of the diffraction pattern obtained on the TOF diffractometer PEARL/HiPr for $CuGe_{0.76}Si_{0.24}O_3$; the crosses designate the data, and the line the calculated profile. Vertical bars indicate the positions of Bragg reflections.

that the effect of Si doping cannot be compared to that of either high pressure or low temperature, in which cell volume reduction is mainly a result of a decrease along the *b* axis.

The Ge/Si-O bond lengths are significantly shortened with respect to the stoichiometric compound, Ge-O1=1.7488(13) Å and Ge-O2=1.7098(13) Å, as expected due to the smaller ionic radius of Si. In contrast, the Cu-O2 bond does not depend on the Si content and the Cu-O1 bond even increases to 2.7946(11) Å . This behavior reflects the observation at high pressures that the covalent Ge-O-bonds are more compressible. Stronger effects are again observed for the bond angles. The angles related to the rotation of the CuO_2 ribbons around the *c* axis are changed by about 1.5°. The ribbons are less parallel in the Si-containing compound; therefore, one may argue that the Si-insertion acts like negative external pressure of about -1.5 GPa. The smaller Si seems to partially relax the mismatch responsible for the strong anharmonic behavior in CGO. The rotation of the ribbons accounts also for the increase of the *b* parameter and the enhanced Cu-O1 bond distance.

The Si insertion yields a lower η angle of 98.33(5)° and an enhancement of δ to 160.95(14)°. These two effects imply an opposite shift of the magnetic interaction. Using the *J*-angle relations from Refs. 13, 14 and 21 one may estimate a 5–20 % smaller average magnetic interaction *J*. However, an analysis of only the bond angles is certainly insufficient for estimating the local *J* in the neighborhood of a Si atom. As argued by Khomskii *et al.*, the Si will disturb the magnetic interaction in both neighboring chains;[33] furthermore, it will favor an in-phase coupling between these two chains in contrast to the out-of-phase coupling between any neighboring chains in the dimerized phase.[13] Therefore, a strong reduction of T_{SP} should be expected.

IV. CONCLUSION

The present neutron powder diffraction studies provide accurate and detailed insight into the structural pressure dependence of CGO up to ~7 GPa. The strongest influence of external pressure involves the orientation of the CuO_2 ribbons which rotate around the *c* axis, being more parallel to *a* at high pressure. This behavior corresponds to the temperature induced anharmonicities and reflects the general structural instability of CGO. The insertion of Si in the structure mainly acts on the same instability and may be compared to a negative pressure.

The pressure-induced structural changes imply an important reduction of the nearest-neighbor coupling parameter by about $\partial J/J\partial P = -0.03 - 0.08$(1/GPa), in agreement with several direct measurements. The small decrease of the Cu-O2-Cu angle η upon pressure seems to be essential in this context. The significant enhancement of the transition temperature itself, which may not be related directly to the value of *J* within the Cross-Fisher theory, seems to be caused by an enhanced frustration ratio at high pressure.

ACKNOWLEDGMENT

The authors are grateful to J. S. Loveday for assistance in the experiments and the data analysis.

[1] M. Hase, I. Terasaki, and K. Uchinokura, Phys. Rev. Lett. **70**, 3651 (1993); M. Hase, I. Terasaki, K. Uchinokura, M. Tokunaga, N. Miura, and H. Obara, Phys. Rev. B **48**, 9616 (1993).

[2] For a recent review, see J. P. Boucher and L. P. Regnault, J. Phys. I **6**, 1939 (1996).

[3] H. Winkelmann, E. Gamper, B. Büchner, M. Braden, A. Revcolevschi, and G. Dhalenne, Phys. Rev. B **51**, 12 884 (1995).

[4] T. Lorenz, U. Ammerahl, T. Auweiler, B. Büchner, A. Revcolevschi, and G. Dhalenne, Phys. Rev. B **55**, 5914 (1997).

[5] H. Takahashi, N. Môri, O. Fujita, J. Akimitsu, and T. Matsumoto, Solid State Commun. **95**, 817 (1995).

[6] S. Katano, O. Fujita, J. Akimitsu, and M. Nishi, Phys. Rev. B **52**, 15 364 (1995).

[7] A. R. G̃oni, T. Zhou, U. Schwarz, R. K. Kremer, and K. Syassen, Phys. Rev. Lett. **77**, 1079 (1996).

[8] P. H. M. van Loosdrecht, J. Zernan, G. Martinez, G. Dhalenne, and A. Revcolevschi, Phys. Rev. Lett. **78**, 487 (1997).

[9] M. Nishi, O. Fujita, J. Akimitsu, K. Kakurai, and Y. Fujii, Phys. Rev. B **52**, R6959 (1995); M. Nishi, K. Kakurai, Y. Fuji, M. Yethirai, D. A. Tennant, S. E. Nagler, J. A. Fernandez-Baca, O. Fujita, and J. Akimitsu, Physica B **241-243**, 537 (1998).

[10] B. Büchner, U. Ammerahl, T. Lorenz, W. Brenig, G. Dhalenne, and A. Revcolevschi, Phys. Rev. Lett. **77**, 1624 (1996).

[11] U. Ammerahl, T. Lorenz, B. Büchner, A. Revcolevschi, and G. Dhalenne, Z. Phys. B **102**, 71 (1997).

[12] K. Fabricius, A. Klümper, U. Löw, B. Büchner, T. Lorenz, G. Dhalenne, and A. Revcolevschi, Phys. Rev. B **57**, 1102 (1998).

[13] M. Braden, G. Wilkendorf, J. Lorenzana, M. Aïn, G. J. McIntyre, M. Behruzi, G. Heger, G. Dhalenne, and A. Revcolevschi, Phys. Rev. B **54**, 1105 (1996).

[14] W. Geertsma and D. Khomskii, Phys. Rev. B **54**, 3011 (1996).

[15] D. M. Adams, J. Haines, and S. Lenard, J. Phys.: Condens. Matter **3**, 5183 (1991).
[16] S. Bräuninger, U. Schwarz, M. Hanfland, T. Zhou, R. K. Kremer, and K. Syassen, Phys. Rev. B **56**, R11 357 (1997).
[17] J. M. Besson, R. J. Nelmes, G. Hamel, G. Weill, J. S. Loveday, and S. Hull, Phys. Rev. B **45**, 2613 (1992).
[18] A. C. Larson, R. B. van Dreele, Los Alamos National Laboratory Report No. LAVR 86748, 1986 (unpublished).
[19] M. Braden (unpublished).
[20] M. Braden, E. Ressouche, B. Büchner, R. Keßler, G. Heger, G. Dhalenne, and A. Revcolevschi, Phys. Rev. B **57**, 11 497 (1998).
[21] B. Büchner, H. Fehske, A. P. Kampf, and W. Wellein, cond-mat/9806022 (unpublished).
[22] R. Werner, C. Gros, and M. Braden, Phys. Rev. B **59**, 14 356 (1999).
[23] M. C. Cross and D. S. Fischer, Phys. Rev. B **19**, 402 (1979).
[24] C. Gros and R. Werner, Phys. Rev. B **58**, R14 677 (1998).
[25] M. Braden, B. Hennion, W. Reichardt, G. Dhalenne, and A. Revcolevschi, Phys. Rev. Lett. **80**, 3634 (1998).
[26] J. Riera and A. Dobry, Phys. Rev. B **51**, 16 098 (1995).
[27] G. Castilla, S. Chakravarty, and V. J. Emery, Phys. Rev. Lett. **75**, 1823 (1995).
[28] W. Brenig, Phys. Rev. B **56**, 14 441 (1997) and references therein.
[29] A. Klümper, R. Raupach, and F. Schönfeld, Phys. Rev. B **59**, 3612 (1999).
[30] S. B. Oseroff, S.-W. Cheong, B. Aktas, M. F. Hundley, Z. Fisk, and L. W. Rupp, Jr., Phys. Rev. Lett. **74**, 1450 (1995).
[31] J. P. Renard, K. LeDang, P. Veillet, G. Dhalenne, A. Revcolevschi, and L. P. Regnault, Europhys. Lett. **30**, 475 (1995).
[32] M. Weiden, R. Hauptmann, W. Richter, C. Geibel, P. Hellmann, M. Köppen, F. Steglich, M. Fischer, P. Lemmens, G. Güntherodt, A. Krimmel, and G. Nieva, Phys. Rev. B **55**, 15 067 (1997).
[33] D. Khomskii, W. Geertsma, and M. Mostovoy, Czech. J. Phys. **46**, 3239 (1996).